

# Theoretical and experimental studies of the atomic structure of oxygen-rich amorphous silicon oxynitride films

W. L. Scopel, Antônio J. R. da Silva, W. Orellana, R. J. Prado, M. C. A. Fantini, and A. Fazzio\*  
*Instituto de Física, Universidade de São Paulo, Caixa Postal 66318, CEP 05315-970, São Paulo, SP, Brazil*

I. Pereyra

*Escola Politécnica, Universidade de São Paulo, Caixa Postal 61548, CEP 05424-970, São Paulo, SP, Brazil*

(Received 27 March 2003; revised manuscript received 30 June 2003; published 28 October 2003)

In this work we used an empirical potential model in order to describe the bulk structure of the oxygen-rich Si-O-N amorphous system. From the atomic configuration obtained by Monte Carlo simulations, the local order structure and the pair correlation function are determined. The results show that the basic structure of the amorphous is well described by a random distribution of tetrahedra with a central Si atom bonded to nitrogen and oxygen atoms. The Fourier transform of the extended x-ray-absorption fine structure (EXAFS) signal obtained by *ab initio* multiple-scattering calculations, using the theoretical atomic structure as input, shows good agreement with the experimental EXAFS analysis performed at the silicon *K* edge.

DOI: 10.1103/PhysRevB.68.155332

PACS number(s): 78.55.Qr, 61.43.Bn, 61.18.-j

## I. INTRODUCTION

The contemporary electronic industry is dominated by silicon. This is the reason why silicon compounds and alloys are under constant investigation by researchers in the area of materials development. In particular, amorphous silicon oxide ( $a\text{-SiO}_2$ ) and amorphous silicon oxynitride ( $a\text{-SiO}_x\text{N}_y$ ) are intensely used in microelectronics<sup>1</sup> and integrated optical supplies.<sup>2</sup> For example, the substitution of  $a\text{-SiO}_2$  by  $a\text{-SiO}_x\text{N}_y$  in ultrathin planar film devices<sup>3-6</sup> was proposed since the N incorporation improves the dielectric properties of the insulator. Another important progress coming from the incorporation of N in silicon oxide is that this compound acts as an efficient barrier against boron diffusion between the gate and the drain in metal-oxide-semiconductor (MOS) devices.<sup>7</sup>

Among the different deposition techniques used to grow silicon oxynitride thin films, the plasma-enhanced chemical vapor deposition (PECVD) technique joins the advantage of low-temperature processing ( $\sim 300^\circ\text{C}$ ) together with a high deposition rate (microns per hour) being a promising alternative to deposit thick films.<sup>8,9</sup> The PECVD technique allows control of a certain number of experimental parameters (rf power, temperature, gas flow, and pressure) which can be easily adjusted to obtain films with specific characteristics for a predetermined application.<sup>10</sup>

The physical properties of  $a\text{-SiO}_x\text{N}_y$  films depend on their atomic composition, morphology, and local structure. In particular, the correlation between local structure and physical properties is of fundamental importance to determine the materials' technological use. Among the experimental methods to investigate the local structure of amorphous multicomponent systems, the x-ray-absorption fine structure (XAFS) method is one of the most appropriate. The soft x-ray absorption at the Si *K* edge was the approach chosen in our work to elucidate the structure of  $a\text{-SiO}_x\text{N}_y$  films deposited by PECVD.<sup>11</sup> Moreover, theoretical simulations can also be a valuable tool to investigate the structure of amorphous ma-

terials. Not only they can help to understand the experimental results, but they can also provide valuable insight that is sometimes hard, or even impossible, to obtain experimentally.

The structure in the EXAFS spectrum is closely related to the local environment of the excited atoms (in this work Si), and a Fourier transform of the oscillations yields a real-space distribution, similar to a radial distribution function. Then, the immediate environment of the Si atoms can be obtained by EXAFS data. In addition, aiming at a better analysis of the structural properties obtained from experimental data, a model of the interatomic potential was developed to describe the bulk structure of oxygen-rich  $a\text{-SiO}_x\text{N}_y$ , by means of Monte Carlo simulations. The oxygen-rich system was chosen because this material does not have Si-OH and Si-H bonds.<sup>11</sup> The presence of these bonds in the oxynitride thin films significantly increases optical losses in the spectral region of interest in optical devices.<sup>12</sup>

## II. EXPERIMENTAL METHOD

The films analyzed in this work were deposited in a PECVD system from a mixture of  $\text{N}_2\text{O}$  and  $\text{SiH}_4$  gases.<sup>11</sup> The  $[\text{N}_2\text{O}/\text{SiH}_4]$  flow ratios (FR) were 2.00 and 3.00. The chemical composition of the film under investigation was determined by Rutherford backscattering spectroscopy (RBS) at LAMFI/USP (São Paulo, Brazil). The RBS data were analyzed by the RUMP (Ref. 13) routine and the atomic concentrations of silicon, nitrogen, and oxygen were obtained. X-ray-absorption spectroscopy (XAS) measurements at the silicon *K* edge were performed to investigate the structural properties of the amorphous samples. The standard samples were  $a\text{-SiO}_2$  (thermally grown) and  $c\text{-Si}$  and  $a\text{-Si}_3\text{N}_4$  (deposited by PECVD). The experiments, performed at room temperature, were carried out at the SXS beamline<sup>14</sup> of the Brazilian Synchrotron Light Laboratory (LNLS, Campinas, Brazil). The measurements were obtained in the energy range of 1800–2300 eV, using a channel-cut InSb (111) monochromator. The detection mode was the total

current yield at the sample's surface. The extended x-ray-absorption fine structure (EXAFS) spectra were collected with a step of 1.0 eV. The EXAFS data obtained experimentally were treated using the software developed by Michalowicz,<sup>15</sup> as described elsewhere.<sup>11</sup>

### III. THEORETICAL METHOD

The atomic simulations, carried out to determine the structural properties (especially local ones) of the oxygen-rich Si-O-N system, were based on the empirical potential models, developed by P. Vashishta and co-workers, to describe the systems SiO<sub>2</sub> (Ref. 16) and Si<sub>3</sub>N<sub>4</sub> (Ref. 17). These effective interatomic potentials include both two- and three-body interactions. The two-body potential includes a steric repulsion term related to the atomic sizes, screened Coulomb interaction caused by the charge transfer effect, and charge-dipole interaction resulting from the large electronic polarizability of O<sup>2-</sup> and N<sup>3-</sup>. The three-body covalent contribution takes into account the bond bending and bond stretching effects. In this work, we introduce two additional contributions to the interatomic potential: (i) a repulsive term to the two-body interactions in order to describe the O-N repulsion and (ii) a three-body interaction to correctly describe the local N-Si-O configuration. The two-body interactions are represented by

$$V_2(r_{ij}) = A \left( \frac{\sigma_i + \sigma_j}{r_{ij}} \right)^{\eta_{ij}} + \frac{Z_i Z_j}{r_{ij}} \exp \left[ -\frac{r_{ij}}{\lambda} \right] - \frac{(\alpha_i Z_j^2 + \alpha_j Z_i^2)}{2r_{ij}^4} \exp \left[ -\frac{r_{ij}}{\xi} \right], \quad (1)$$

and the three-body interactions take the following form:

$$V_3(r_{ij}, r_{ik}) = B_{ijk} \left[ \frac{\vec{r}_{ij} \cdot \vec{r}_{ik}}{r_{ij} r_{ik}} - \cos \bar{\theta}_{ijk} \right]^2 \exp \left[ \frac{\mu}{r_{ij} - r_0} + \frac{\mu}{r_{ik} - r_0} \right]. \quad (2)$$

To avoid a discontinuous two-body potential caused by its truncation at  $r = r_c$ , we replace  $V_2(r_{ij})$  by

$$V_2(r_{ij}) = V_2(r_{ij}) - V_2(r_c) - (r_{ij} - r_c) \left[ \frac{dV_2(r_{ij})}{dr_{ij}} \right]_{r=r_c}. \quad (3)$$

The parameters defined in the potential, such as ionic radii  $\sigma_i$ , repulsive exponents  $\eta_{ij}$ , repulsive strength  $A$ , effective charge  $Z_i$ , polarizabilities  $\alpha_i$ , strength of the three-body interaction  $B_{ijk}$ , average bond angles  $\bar{\theta}_{ijk}$ , and the cutoff distances ( $r_0, r_c, \lambda$ , and  $\xi$ ) for the two-body and three-body interactions are displayed in Table I.

The silicon oxynitride films deposited by PECVD under investigation have a small amount of hydrogen (less than 4%). Moreover, as these H atoms are not bonded to Si atoms<sup>11</sup> and, as we are, in the present work, mostly interested in the analysis of the Si first neighborhood, we will not consider explicitly the H atoms in our simulations. However, the amount of N and O atoms in the simulations will reflect the fact that N-H bond are experimentally observed. We ex-

TABLE I. Parameters used in the interatomic potential for the Si-O-N system.

A (eV)	$\mu$ (Å)	$\lambda$ (Å)	$\xi$ (Å)	$r_0$ (Å)	$r_c$ (Å)
1.592	1.00	4.43	2.50	2.60	5.50
	$\sigma_i$ (Å)		$Z_i$ (e)		$\alpha_i$ (Å) <sup>3</sup>
	Si	0.47	1.76		0.00
	O	1.20	-0.88		2.40
	N	1.30	1.104		3.00
	$\eta_{ij}$				
	Si-Si	11			
	Si-O	9			
	O-O	7			
	Si-N	9			
	N-N	7			
	O-N	7			
	$B_{ijk}$ (eV)		$\bar{\theta}_i$ (deg)		
	O-Si-O	4.993	109.47		
	Si-O-Si	19.972	141.00		
	N-Si-N	4.993	109.47		
	Si-N-Si	12.480	120.00		
	O-Si-N	4.993	109.47		

plored the structural properties of amorphous  $a$ -SiO<sub>x</sub>N<sub>y</sub> through the continuous Monte Carlo (MC) method,<sup>18</sup> using a simulation box with periodic boundary conditions, in the  $N$ - $P$ - $T$  ensemble. In order to generate an amorphous atomic arrangement, we started our simulation from a crystalline structure of silicon nitride (supercell parameters:  $a = b = 15.19$  Å;  $c = 31.922$  Å; density = 2.78 g/cm<sup>3</sup>; 616 atoms). This silicon nitride system is fully melted, and we then randomly replaced nitrogen atoms by oxygen atoms up to the desired atomic concentrations, as determined by RBS for FR = 2.0 (3.0), we end up with 190 (186) Si, 278 (312) O, and 74 (38) N atoms. The system was heated up to the temperature of 7000 K (60 000 MC steps—a MC step is completed after we attempted to displace all the atoms in the system) and it was equilibrated by 90 000 MC steps at this temperature. This procedure guarantees that the initial state has no effect on the final result. Then, the system was cooled from 7000 K down to 6000 K in 30 000 MC steps and equilibrated for another 30 000 MC steps. This cooling was repeated until a configuration at 1000 K was obtained. From 1000 K the system was cooled down to 800 K in 30 000 MC steps and equilibrated by another 30 000 MC steps. Using a similar cooling schedule, a system at 400 K was obtained. Finally, the system was brought down from 400 K to 300 K in 30 000 MC steps, with a final equilibration period of 30 000 MC steps.

It should be mentioned that the ideal procedure to generate the amorphous structure would be to perform *ab initio* calculations. However, the size of the system used in the present study, coupled to the large number of energy evaluations that are required to generate the amorphous structure, prevents such an approach. Moreover, tight-binding (TB)

calculations, which could also be an alternative, cannot be carried out for this system owing to the lack of a suitable parametrization. Nevertheless, even though the use of empirical potentials is almost unavoidable (for the reasons mentioned above), one must keep in mind the limitations of this approach. However, as will be seen below, the good agreement between the experimental and theoretical results gives us confidence that the potential is describing, at least the local order structure, correctly.

### RESULTS OF THE CHEMICAL AND STRUCTURAL PROPERTIES OF AMORPHOUS $\text{SiO}_x\text{N}_y$

The RBS results show that the samples, deposited with  $\text{FR}=2.00$  and  $3.00$ , have the following atomic concentrations: 36% Si, 50% O, and 14% N and 36% Si, 57% O, and 7% N, respectively. Thus, these results indicate that the silicon oxynitride films are oxygen rich.

The XANES spectra<sup>11</sup> of the samples under investigation show that their short-range structures are similar to that of amorphous  $\text{SiO}_2$ . Moreover, the Fourier transform (FT) of the EXAFS signal shows that this short-range structure is of the order of 3 Å. In silicon oxynitrides, the Si atoms tend to be tetrahedrally coordinated, each O atom has two Si atoms as nearest neighbors, and each N atom has coordination 3. For the analysis of the EXAFS data, we considered that in the first coordination shell the silicon atoms are connected to oxygen and nitrogen atoms, because these bonds are evidenced in the Fourier transform infrared spectroscopy (FTIR) spectra.<sup>11</sup> The EXAFS results show that the average interatomic distances are ( $d_{\text{Si-O}}=1.61\pm 0.02$  Å) and ( $d_{\text{Si-N}}=1.70\pm 0.02$  Å). The EXAFS analysis also shows that the average oxygen and nitrogen coordination numbers around the silicon atoms are  $N_{\text{Si-O}}=2.75$  and  $N_{\text{Si-N}}=1.25$ , for the sample  $\text{FR}=2.00$ , and  $N_{\text{Si-O}}=3.20$  and  $N_{\text{Si-N}}=0.80$ , for the sample  $\text{FR}=3.00$ . The sum of  $N_{\text{Si-O}}$  and  $N_{\text{Si-N}}$  equals 4, the total number of Si first neighbors, as expected.<sup>19</sup>

Even though the experimental analysis gives an overall qualitative idea about the structure of the samples, it does not provide a detailed atomic configuration. Experimental limitations, together with the amorphous nature of the material, restrict the reliable structural information to the immediate neighborhood of the Si atoms. The MC simulations can help to bridge this gap. Therefore, we have performed MC simulations, as described in the previous section, for atomic concentrations that are equivalent to the experimental samples. The final geometric structure (MC simulation) of the alloy, with atomic concentration identical to the sample deposited with  $\text{FR}=2.00$ , is depicted in Fig. 1.

These atomic positions (MC simulation,  $\text{FR}=2.00$ ) were used to determine the theoretical FT. The results were compared with the experimental data, already published.<sup>11</sup> The theoretical EXAFS signal was obtained using the FEFF8 software,<sup>20</sup> having as input the atomic structure generated through the MC simulation. The FEFF8 makes *ab initio* multiple-scattering calculations of XAFS spectra for clusters of atoms. The calculations used a cluster of 60 atoms at the center of the supercell determined by the MC calculations. The number of multiple scattering paths was taken as 4, and

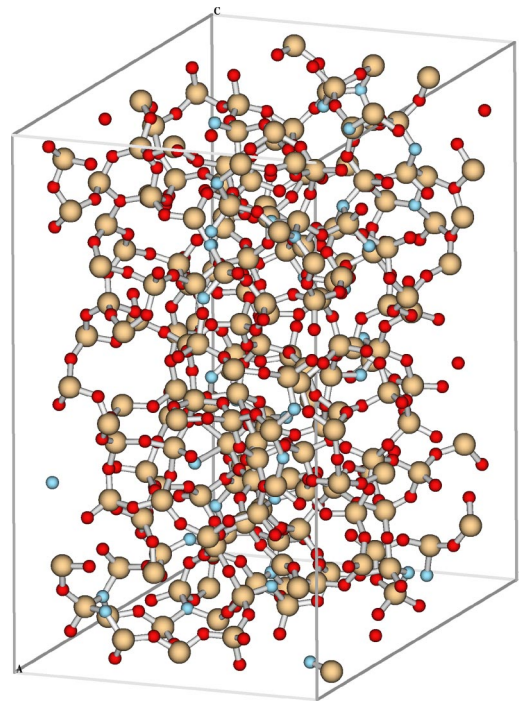


FIG. 1. Geometric structure obtained using the simulation procedure described in the text, for an atomic concentration similar to the sample ( $\text{FR}=2.00$ ). This supercell is repeated in space using periodic boundary conditions. The gray spheres represent N (smaller) and Si (larger) atoms. The black spheres represent O atoms.

the maximum distance to the absorbing Si atom as 9 Å. The absorption function was obtained considering the Si  $K$  edge and taking an average over these 60 atoms. The calculations were performed at the same conditions used to analyze the experimental data.<sup>11</sup> The comparison between the FT of the EXAFS signal obtained theoretically (as described above) and experimentally (as described in Ref. 11) is shown in Fig. 2.

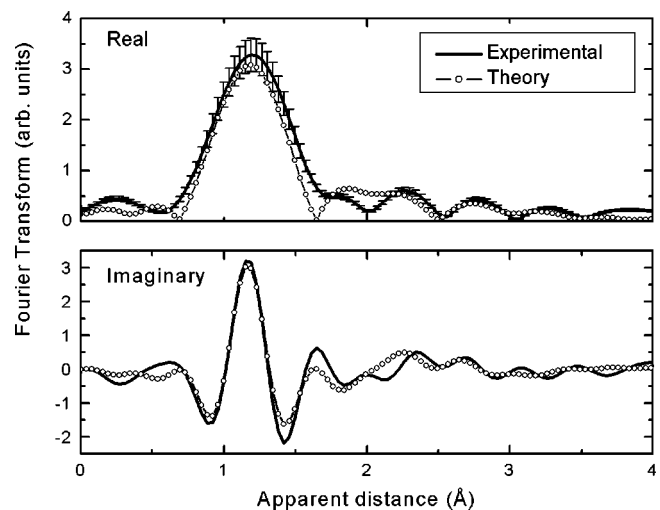


FIG. 2. Comparison between the Fourier transforms of the EXAFS signal obtained experimentally and theoretically (FEFF8).



Figure 2 shows a nearly quantitative agreement between (1) the FT obtained by the FEFF8 software plus the theoretical structure and (2) the FT of the EXAFS experimental results for both the real and imaginary parts. The discrepancies observed in the range 1.5–2.5 Å can be described as an overlap between the second and third coordination shells in the theoretical spectrum, when compared to the experimental results. A possible cause of this discrepancy is the finite number of atomic clusters used to calculate the theoretical FT with FEFF8. The long-range structure of the amorphous system would be better described by taking a larger number of clusters, as well as longer distances to the silicon absorber, thus generating a better EXAFS signal by multiple-scattering calculations. Nevertheless, since the most relevant structural information of amorphous systems is the first coordination shell, the comparison between theory and experiment in our approach provides consistent conclusions. In particular, the peak with large magnitude around 1.30 Å is associated with the first coordination shell, which is formed by Si-O and Si-N bonds. Thus, the atomic short-range order generated by the MC simulation is being well described when compared to the experimental results. Moreover, the absence of long-range order is evident at distances larger than 3 Å, confirming that the Si-O-N system is amorphous.

From a morphological point of view, the theoretical result of Fig. 1 reveals that the amorphous Si-O-N system is homogeneous and is not composed by two distinct phases SiO<sub>2</sub> and Si<sub>3</sub>N<sub>4</sub>. One can also see, as expected, that the first neighbors of silicon are oxygen and nitrogen atoms. Moreover, there are silicon atoms connected to (i) four oxygens, (ii) three oxygens and one nitrogen, (iii) two oxygens and two nitrogens, and (iv) one oxygen and three nitrogens, in both systems characterized by FR=2.00 and FR=3.00.

On the other hand, our experimental results, published in Ref. 11, evidenced the formation of a disordered Si-O-N structure, in which the silicon atoms are fourfold coordinated with N and/or O in the first shell. These experimental results are a combination of RBS, XAS, and FTIR data, and as discussed in detail in Ref. 11, they clearly show that the material is not composed of SiO<sub>2</sub> and Si<sub>3</sub>N<sub>4</sub> regions, but of a homogeneous system with randomly distributed Si-O and Si-N bonds. By randomly distributed, we do not mean that there will be the same number of Si-N and Si-O bonds, since the concentrations of O and N atoms are not the same. All these experimental results suggest, as a reasonable picture to describe the local structure, the so-called random bond model (RBM).<sup>21</sup> In the RBM, there are five types of nearest neighborhoods around the Si atoms or five types of tetrahedra SiO<sub>ν</sub>N<sub>4-ν</sub>, where ν=0, 1, 2, 3, or 4. For example, if ν=2, it means that the silicon is connected to two oxygen and two nitrogen atoms. According to the RBM, the relative probabilities of these five types of tetrahedra are determined as

$$W(x,y) = \left[ \frac{2x}{2x+3y} \right]^\nu \left[ \frac{3x}{2x+3y} \right]^{4-\nu} \frac{4!}{\nu!(4-\nu)!}, \quad (4)$$

where  $x$  and  $y$  are the *experimentally* determined atomic ratios [O]/[Si] and [N]/[Si], respectively, obtained from the

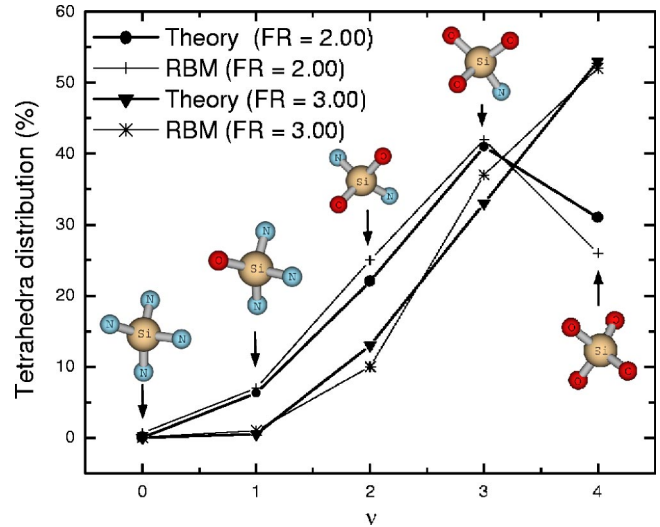


FIG. 3. Statistical distribution of tetrahedral configurations, obtained from the MC simulations and the RBM, as a function of  $\nu$ , where  $\nu$  is related to the five types of tetrahedra SiO<sub>ν</sub>N<sub>4-ν</sub> ( $\nu = 0, 1, 2, 3$ , and 4). For example, if  $\nu=2$ , it means that the silicon is connected to two oxygen and two nitrogen atoms. The gray spheres represent N (smaller) and Si (larger) atoms. The black spheres represent O atoms.

RBS data (see Fig. 3). These probabilities can be used to calculate the number of oxygen and nitrogen atoms bonded to silicon, in the first coordination shell. It is important to note that the values obtained for  $N_{Si-O}$  and  $N_{Si-N}$  in this way are very similar to the ones *independently obtained* from the XAS results (see above), within an uncertainty of 10%,<sup>11</sup> which gives further confidence that the RBM is correct. From the MC simulation, we can also extract the statistical distribution of these tetrahedra (using a cutoff distance of 1.7 Å to determine the nearest neighbors to the Si atoms), which is also shown in Fig. 3. From this figure, it can be seen that the agreement between the MC and RBM results is very good. It is important to remark that these results were obtained independently, as previously described. Therefore, the facts that (1) the MC simulations describe well the first neighborhood around the Si atoms, as established above (Fig. 2), and (2) there is the nice agreement shown in Fig. 3 are strong indications that the RBM is describing well the local structure of the amorphous system.

The distinct partial pair-distribution functions  $g_{AB}(r)$  between atoms  $A$  and  $B$  of the theoretically obtained amorphous Si-O-N system, equivalent to the sample deposited with FR=2.00, are shown in Fig. 4. From this figure, the positions of the first peaks in  $g_{Si-O}$  and  $g_{Si-N}$  are determined as  $(1.60 \pm 0.04)$  and  $(1.71 \pm 0.06)$ , respectively. These values for the average interatomic distances  $d_{Si-O}$  and  $d_{Si-N}$  are consistent with our experimental EXAFS data, as well as those in the literature.<sup>22</sup> From the area under the first peak, the nearest-neighbor coordination number of O is found to be 2 and of N it is found to be 2.54, for the simulated sample FR=2.00. It should be stressed that we are not implying with this result that the N atoms would have, *in the real material*, a coordination number smaller than 3. In the experimental amorphous system, there is an incorporation of

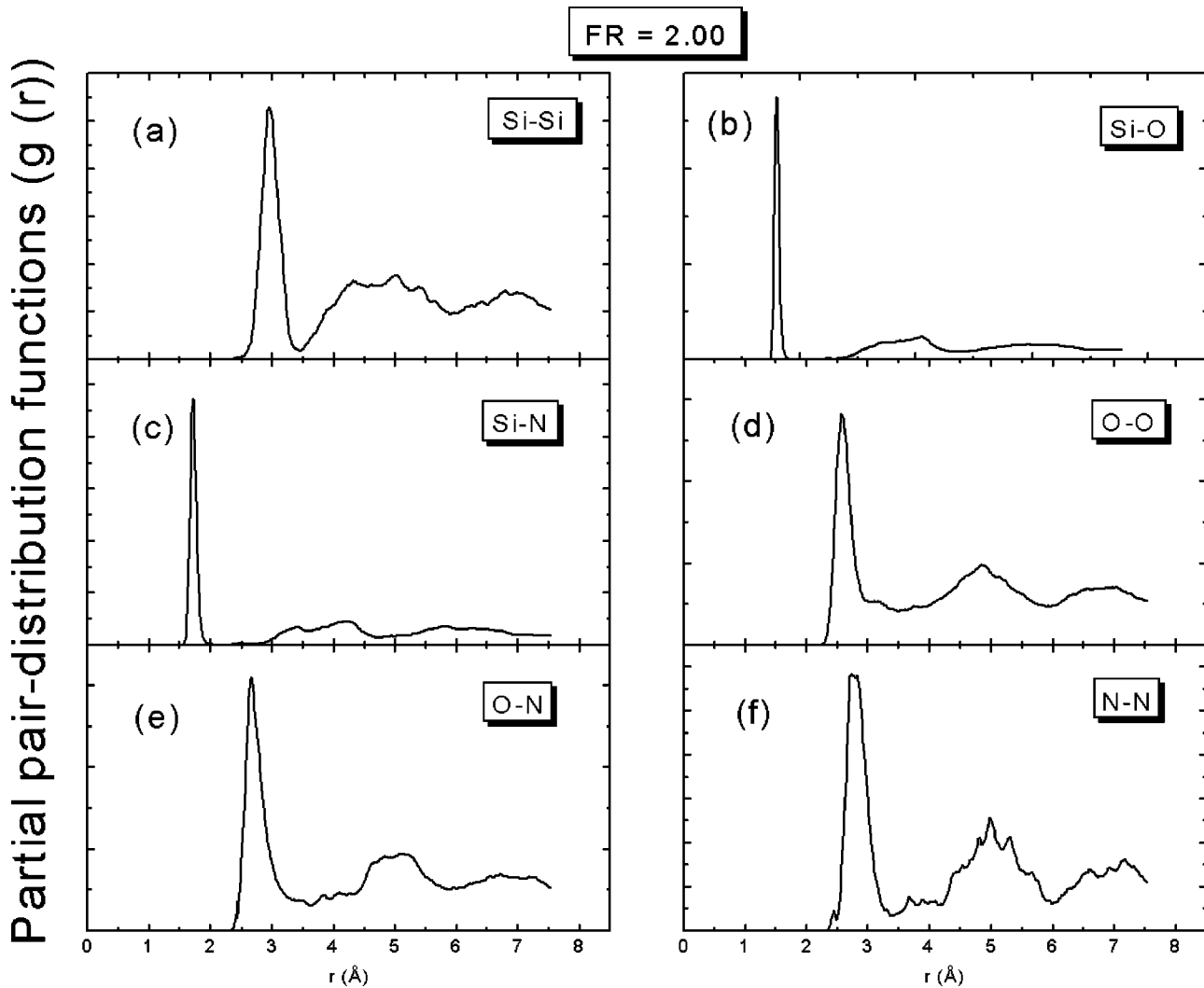


FIG. 4. Pair-distribution functions for the MC structure simulating the FR=2.00 sample, for a temperature of 300 K.

hydrogen atoms in the samples deposited by PECVD, manifested through the detection of N-H bonds,<sup>11</sup> as already mentioned. The number of N atoms that were considered in the simulation already reflect this fact: considering that we have 190 Si, 278 O, and 74 N atoms and assuming that all the Si atoms are four-fold coordinated and all the O atoms are two-fold coordinated, the maximum N coordination number would be 2.76. It is not exactly 3 here because some of the N atoms in the real system<sup>23</sup> are making N-H bonds, a fact that was implicitly included in the simulation (through the number of N atoms). In conclusion, the fact that the nitrogen coordination has a value smaller than 3 in our simulations is not a problem with our potential, but is a consequence of the fact that there are no H atoms in our theoretical procedure to saturate the “N dangling bonds,” as opposed to the real samples where, as mentioned above, there are N-H bonds present. Finally, the reason that the N coordination number is smaller than 2.76 is related to a small number of Si atoms that do not have a coordination number of 4 (considering only N and O atoms).

From Fig. 4, we obtain for the average nearest-neighbor distances between O-O, O-N, N-N, and Si-Si the values 2.57

$\text{\AA}$ , 2.66  $\text{\AA}$ , 2.80  $\text{\AA}$ , and 2.95  $\text{\AA}$ , respectively. The O-O and Si-Si bond lengths present a small shift of  $\approx 5\%$  when compared to other simulations of the *a*-SiO<sub>2</sub> material.<sup>24</sup> On the other hand, the O-N and N-N average bond lengths are consistent with other experimental works.<sup>22</sup>

#### IV. CONCLUSIONS

In this work we have performed MC simulations of oxygen-rich amorphous Si-N-O systems in order to obtain an insight into their atomic structure. To perform these simulations we have extended empirical interatomic potentials that were previously developed to study SiO<sub>2</sub> and Si<sub>3</sub>N<sub>4</sub>. The comparison between experiment and theory, in particular the nice agreement between the FT of the EXAFS signal obtained theoretically and experimentally, indicates that, as a first approximation, our developed model of interatomic potentials works satisfactorily well for the short-range order, not only with respect to the distribution of different kinds of Si nearest-neighbor atoms, but also with respect to their distances. Also, the MC simulations help to confirm that the

amorphous structure appears to be formed by a random mixture of silicon atoms bonded to oxygen and nitrogen, as evidenced by the good agreement between the statistical distributions of the five types of tetrahedra obtained using the MC results and the RBM.

## ACKNOWLEDGMENTS

Thanks are due to the Brazilian agencies FAPESP and CNPQ for financial support and LNLS-Brazil for the XAS measurements.

\*Electronic address: fazzio@if.usp.br

- <sup>1</sup>R. Chau, J. Kavalieros, B. Roberts, R. Schenker, D. Lionberger, D. Barlage, B. Doyle, R. Arghavani, A. Murthy, and G. Dewey, *Tech. Dig. Int. Electron Devices Meet.* **2000**, 45 (2000).
- <sup>2</sup>M. Hoffman, P. Koka, and E. Voges, *J. Lightwave Technol.* **16**, 395 (1998).
- <sup>3</sup>D.A. Buchanan, *IBM J. Res. Dev.* **43**, 245 (1999).
- <sup>4</sup>C.S. Mian and I.S. Flora, *Solid-State Electron.* **43**, 1997 (1999).
- <sup>5</sup>T.M. Pan, T.F. Lei, and T.S. Chao, *IEEE Electron Device Lett.* **21**, 378 (2000).
- <sup>6</sup>S. Bernerjee, A. Gibaud, D. Chateigner, S. Ferrari, and M. Fanciulli, *J. Appl. Phys.* **91**, 540 (2002).
- <sup>7</sup>K.A. Ellis and R.A. Buhrman, *Appl. Phys. Lett.* **69**, 535 (1996).
- <sup>8</sup>M.I. Alayo, I. Pereira, and M.N.P. Carreño, *Thin Solid Films* **332**, 40 (1998).
- <sup>9</sup>I. Pereira and M.I. Alayo, *J. Non-Cryst. Solids* **212**, 225 (1997).
- <sup>10</sup>C. Domínguez, J.A. Rodríguez, F.J. Muñoz, and N. Zine, *Vacuum* **52**, 3 (1999); A.H. Teller and E. Teller, *J. Chem. Phys.* **21**, 1087 (1953).
- <sup>11</sup>W.L. Scopel, M.C.A. Fantini, M.I. Alayo, and I. Pereyra, *Thin Solid Films* **413**, 59 (2002).
- <sup>12</sup>K. Worhoff, A. Driessen, P.V. Lambeck, L.T.H. Hilderink, P.W.C. Linders, and T.J.A. Popma, *Sens. Actuators A* **74**, 9 (1999).
- <sup>13</sup>L.R. Doolittle, *Nucl. Instrum. Methods Phys. Res. B* **9**, 344 (1985).
- <sup>14</sup>M. Abbate, F.C. Vicentin, V. Compagnon-Cailhol, M.C. Rocha, and H. Tolentino, *J. Synchrotron Radiat.* **6**, 964 (1999).
- <sup>15</sup>A. Michalowicz, *EXAFS pour le Mac*, Logiciels por la Chimie (Société Française de Chimie, Paris, 1991), p. 102.
- <sup>16</sup>A. Nakano, R.K. Kalia, and P. Vashista, *J. Non-Cryst. Solids* **171**, 157 (1994).
- <sup>17</sup>P. Vashishta, R. K. Kalia, W. Li, and I. Ebbsjo, in *Amorphous Insulators and Semiconductors*, edited by M. F. Thorpe and M. I. Mitkova (Kluwer, Dordrecht, 1996).
- <sup>18</sup>P.P.M. Venezuela and A. Fazzio, *Phys. Rev. Lett.* **77**, 546 (1996).
- <sup>19</sup>In a first step of the EXAFS analysis, the Si coordination number was constrained to be 4. However, later on, this constraint was removed.
- <sup>20</sup>J.J. Rehr, R.C. Albers, C.R. Natoli, and E.A. Stern, *Phys. Rev. B* **34**, 4350 (1986).
- <sup>21</sup>H.R. Philipp, *J. Non-Cryst. Solids* **8–10**, 627 (1972).
- <sup>22</sup>K.M. Behrens, E.D. Klinkenberg, J. Finster, and K.H. Meiwes-Broer, *Surf. Sci.* **402–404**, 729 (1998).
- <sup>23</sup>M.I. Alayo, I. Pereira, W.L. Scopel, and M.C.A. Fantini, *Thin Solid Films* **402**, 154 (2002).
- <sup>24</sup>P. Vashishta, R.K. Kalia, J.P. Rino, and I. Ebbsjo, *Phys. Rev. B* **41**, 12 197 (1990).